Sustained high winter glacier velocities from brief warm events

Léo Decaux[1,1], Kenneth D Mankoff[2,2], Mariusz Grabiec[3,3], Joanna Tuszynska[1,1], Bartłomiej Luks[4,4], Jacek Adam Jania[3,3], and Andreas Alexander[5]

[1]University of Silesia in Katowice, Faculty of Natural Sciences, Institute of Earth Sciences
[2]Geological Survey of Denmark and Greenland
[3]University of Silesia in Katowice
[4]Institute of Geophysics, Polish Academy of Sciences
[5]University of Oslo

November 30, 2022

Abstract

A single week-long warm event in midwinter in Svalbard flooded an inefficient en- and subglacial drainage system and led to a 2.5x velocity increase that remained in effect for the remainder of the winter - more than 3 months. Because of the long winter season, changes in winter velocity have a large impact on the annual average velocity. As the climate warms and surface melt and rain events increase during winter months, sustained high winter glacier velocities are likely to occur more often. Increasing glacier velocity near the terminus leads to additional ice entering the fjord, and an increase of ice dynamics contribution to sea level rise during winter.

Posted on 30 Nov 2022 | CC-BY-NC-ND 4 | https://doi.org/10.1002/essoar.10506915/v2 | This a preprint and has not been peer reviewed. Data may be preliminary.

Sustained high winter glacier velocities from brief warm events

Léo Decaux [1], Kenneth D. Mankoff [2,3], Mariusz Grabiec [1], Andreas Alexander [4], Joanna Tuszynska [1], Bartłomiej Luks [5]and Jacek Jania [1]

[1]University of Silesia in Katowice, Faculty of Natural Sciences, Institute of Earth Sciences, Bedzinska 60, 41-200 Sosnowiec, Poland
[2]National Snow and Ice Data Center, University of Colorado, Boulder, CO 80309 USA
[3]Department of Glaciology and Climate, Geological Survey of Denmark and Greenland (GEUS), Øster Voldgade 10, DK-1350, Copenhagen K, Denmark
[4]Department of Geosciences, University of Oslo, 0316 Oslo, Norway
[5]Institute of Geophysics, Polish Academy of Sciences, Ksiecia Janusza 64, 01-452 Warsaw, Poland

Key Points:

- A single week-long warm event in the winter can lead to a more than doubling of the velocity of the glacier for more than 3 months

Corresponding author: Léo Decaux, `leodecaux@gmail.com`

Abstract

A single week-long warm event in midwinter in Svalbard flooded an inefficient en- and subglacial drainage system and led to a 2.5x velocity increase that remained in effect for the remainder of the winter - more than 3 months. Because of the long winter season, changes in winter velocity have a large impact on the annual average velocity. As the climate warms and surface melt and rain events increase during winter months, sustained high winter glacier velocities are likely to occur more often. Increasing glacier velocity near the terminus leads to additional ice entering the fjord, and an increase of ice dynamics contribution to sea level rise during winter.

Plain Language Summary

Most glacial field studies occur in summer due to the difficulties of winter polar fieldwork. However, because of this long Arctic winter season, changes in the winter ice speed can cause large changes in annual average speed. The causes of these changes are generally well-understood and linked to water inputs to the inside and the base of the glacier. We installed a pressure transducer in an ice cave, and combined with a model, weather stations, and GPS measuring ice speed, we show that a single week-long warm event in the winter led to a more than doubling of the winter velocity for more than 3 months. In a warming climate, more winter melt and rain is likely to occur, and may lead to increased winter glacier velocity, additional ice entering fjords, and increased rates of sea level rise.

1 Introduction

Glacier velocity changes are primarily driven by internal drainage system (IDS) hydrologic changes (Anderson et al., 2004; Bingham et al., 2006; Brinkerhoff et al., 2016; Hooke et al., 1997; Iken & Bindschadler, 1986; Jansson, 1995; Mair et al., 2003; Willis, 1995). In the spring, warming atmospheric temperatures start melting the glacier surface, and snowfall becomes rain. As the meltwater and rain enters an inefficient subglacial system, effective basal pressure decreases and ice velocity increases. Eventually, larger volumes of basal water carve large subglacial channels that efficiently exhaust the water, and a mid-to-late summer slowdown may occur. Minimum velocity is often in the early fall when the surface runoff stops and water leaves the subglacial system more quickly than the creep closure of the large subglacial conduits, leading to high effective pressure. Throughout the winter, velocity starts to increase again as subglacial conduits shrink and decrease the effective basal pressure. There may also be some delayed water from the upper part of the glacier that impacts winter velocity (Joughin et al., 2008; Stevens et al., 2016; Vijay et al., 2019).

Overlaid on the seasonal cycle, short-term velocity increases are generally associated with lake drainage, rain, or excessive warm events – all of which can generate sufficient surface meltwater that, when delivered to the bed, can temporarily overwhelm even large subglacial channels (Anderson et al., 2014; Bartholomaus et al., 2008; Doyle et al., 2015; Hart et al., 2019; Schoof, 2010).

Because the IDS is less efficient in the winter or early spring, less water is needed in these seasons to fill it, overwhelm it, and cause an ice dynamics response. This property is the cause of spring velocity spikes observed on temperate and polythermal glaciers and ice sheets (Bingham et al., 2006; I. Hewitt, 2013; Kessler & Anderson, 2004; Mair et al., 2003), and why many surge events, correlated with high basal water pressures, start in winter (Harrison & Post, 2003; Kamb et al., 1985; Lingle & Fatland, 2003; Sund et al., 2014).

Although glacier studies usually occur during summer months, likely due to the difficulties of Arctic winter fieldwork, there is an increasing body of literature highlighting the importance of variability in winter motion (e.g., Burgess et al., 2013; Hart et al., 2019; Schoof et al., 2014; Sole et al., 2013). Because the Arctic winter (and associated slower glacier velocities) is longer than the Arctic summer (and associated glacier velocity increase), an increase in winter ice velocity can have a disproportionately large increase in annual average ice velocity.

Here we add to the growing body of winter velocity studies by presenting a time series of 2016 and 2017 winter observations at a polythermal high Arctic glacier. Data include water level from inside an englacial channel, velocity measurements of the glacier surface, automatic weather station (AWS) data, remote sensing synthetic aperture radar (SAR) images of the glacier surface, and a regional short-range high-resolution weather model.

2 Study area

Hansbreen is a 15.6 km long polythermal tidewater glacier, with a mean ice thickness of 171 m (Grabiec et al., 2012), situated at 77° 04'N, 15° 38'E in southwest Spitsbergen (Figure 1a). It flows towards the south, extending from 664 m altitude to sea level, with a ca. 150 m yr^{-1} velocity at the terminus and a 55–70 m yr^{-1} velocity 3.7 km upstream (Błaszczyk et al., 2009). It is climatically, environmentally, and glaciologically similar to other Svalbard tidewater glaciers (Grabiec et al., 2012; Hagen et al., 1993, 2003). In the past, water level measurements have been collected directly from within its moulins (Schroeder, 1998a, 2007; Vieli et al., 2004) indirectly via ground-penetrating radar (GPR) (Jania et al., 2005), and there have been several en- and sub-glacial explorations quantifying bed properties (Benn et al., 2009; Chen et al., 2018; Gulley et al., 2012, 2014; Mankoff et al., 2017)

This study focuses on measurements from inside an englacial system called Crystal Cave (CC, Figure 1), which has been active since at least 1967 (Benn et al., 2009; Turu, 2012; Schroeder, 1998a, 1998b). Crystal Cave is know to recharge from four moulins and may be occasionally supplied during high discharge events by one additional moulin and one supraglacial stream (Figure 1b) flowing at the interface of the Tuva nunatak and the Tuvbreen glacier (Figure 1a). A subglacial model shows the presence of a subglacial channel nearby CC's entrance (Decaux et al., 2019) and GPR measurements confirm its connection with the subglacial drainage network (Pälli et al., 2003).

3 Methods

3.1 Velocity

We measured velocity with a Global Navigation Satellite Systems (GNSS) receiver Leica Geosystems GPS1200 (L1/L2), that sampled every 3 hours at stake 4MONIT (Figure 1a). Daily speed was calculated from daily displacement of the stake. We define the baseline velocity as the mean velocity from December 1 2016 through February 1 2017.

The velocity has also been surveyed for decades at a stake network along Hansbreen's center line (stakes 2 through 11 in Figure 1a) but with a lower temporal resolution. GNSS positions were recorded (with the same receiver model as at stake 4MONIT) weekly for stakes 2 through 5, and monthly for stakes 6 through 11, depending on weather conditions. The minimum observation time at those stakes is between 20 and 30 minutes. Speed is reported in meter per day even when measured over longer time periods.

Post-processing of all GNSS measurements is done at the Polish Polar Station with Leica Geo Office software by using the reference station (Leica GRX1200 Pro) located

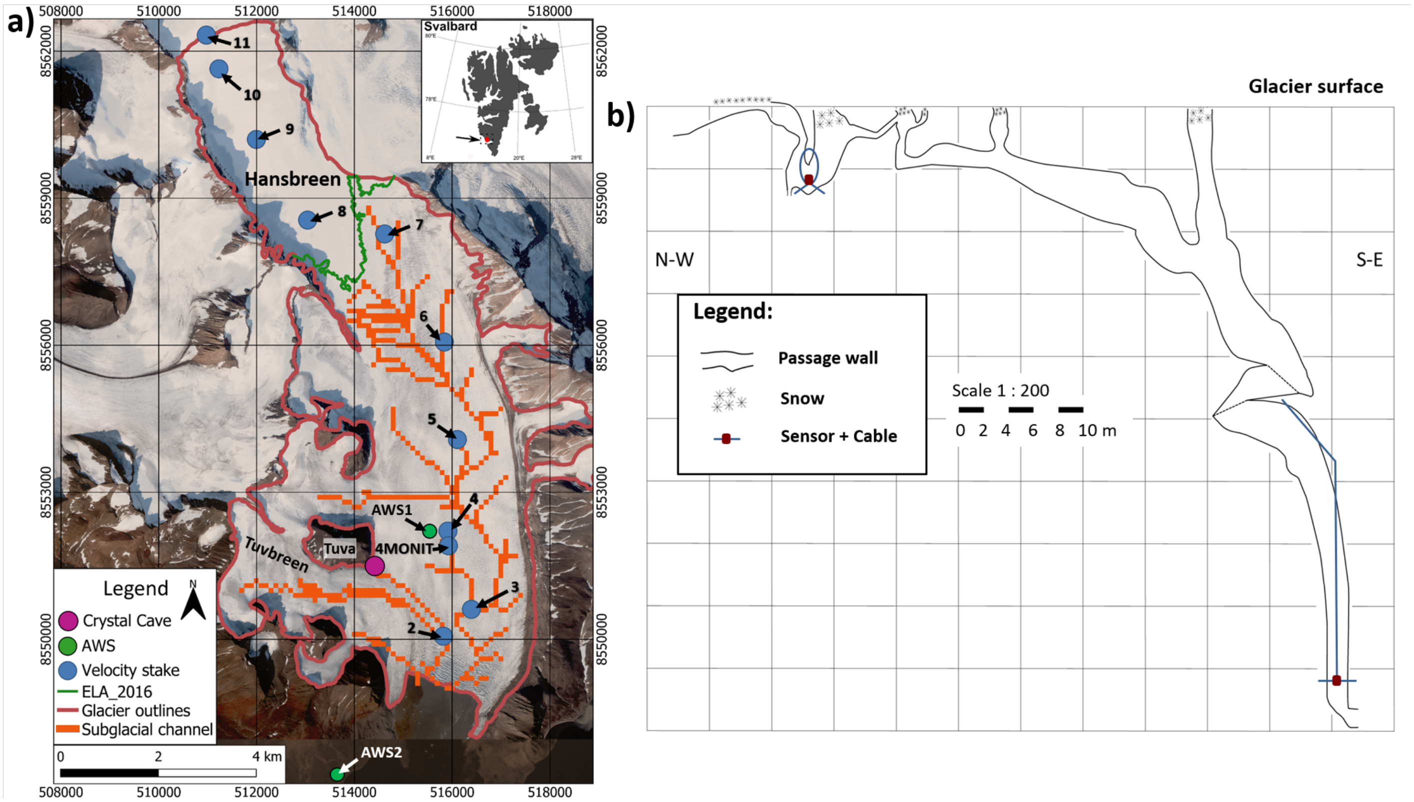

Figure 1. (a) Map showing the locations of the glacier Hansbreen in Svalbard (insert map), the two automatic weather stations (AWS), the 10 velocity stakes, Crystal Cave, subglacial channels from Decaux et al. (2019) and the ELA for 2016 (the accumulation area being above the ELA and ablation area being below the ELA). The background map is an WorldView-2 satellite image acquired on 21 August 2015 combined with an ASTER satellite image acquired on 17 August 2020 and the coordinate system used is WGS 1984 UTM zone 33N. (b) Vertical profile of englacial channel Crystal Cave from April 2017 with sensors locations.

at the Polish Polar Station. The estimated error is between ± 0.025 - 0.005 m day^{-1} and is more than an order of magnitude lower than our measurements.

3.2 Englacial water pressure

Englacial water pressure was recorded by placing HOBO 250-Foot Depth Water Level Data Loggers inside the the Crystal Cave system (Figure 1b). Data loggers recorded pressure and temperature every 30 minutes, have a resolution of 2.55 kPa for a typical error of 3.8 cm water level, and were resampled to daily average values in post-processing.

Sensors were placed in vertical sections of the cave by drilling anchor points into the ice roof above the vertical shaft, then hanging cables down in the center of conduit (Figure 1b). Stabilization cables were used to keep sensors from attaching to and freezing into ice walls by attaching the sensor to three horizontal cables anchored into the ice walls at ca. 120 degrees apart. Although we installed two sensors in CC using this method, the upper one was quickly buried due to the cave surface melting down and drifting snow (Figure 1b).

Here, we report data from the lower senor installed in CC 28 m above the glacier bed (measured) and 46 m below the ice surface (estimated) (Figure 1b) in ice estimated to be 74 m thick. We calculate the flotation fraction k as the ratio between water pressure (P_w) and ice overburden pressure (P_i) (Flowers & Clarke, 1999) following equation 1 and 2:

$$k = \frac{P_w}{P_i}, \tag{1}$$

with:

$$P_w = \rho_w g z_w \quad and \quad P_i = \rho_i g z_i, \tag{2}$$

where ρ_w is the water density (1000 kg m^{-3}), ρ_i is the ice density (917 kg m^{-3}), g is the acceleration due to gravity (9.81 m s^{-2}), z_w and z_i are respectively water level above the bedrock (measured in the cave in m) and ice thickness (74 m).

3.3 Weather

3.3.1 Observed

A nearby weather station, 1.8 km away from CC, provides air temperature from the glacier surface at ca. 165 m a.s.l (AWS1 in Figure 1a). Air temperature, sampled every 10 minutes with ±0.1° C accuracy, comes from a Campbell Scientific 107, and is averaged to daily resolution in post-processing. Precipitation measurements were made at AWS2 at ca. 10 m a.s.l (Figure 1a), located at the Polish Polar Station ca. 1.6 km from the glacier front, with a Hellmann rain gauge D-200 that measured both solid and liquid precipitation. Results were converted into liquid water equivalent in millimeters. Because the measurements are carried out at 0600 UTC+1, the precipitation day is defined as beginning at 0600 UTC+1 on the observed day and ending 0600 UTC+1 on the day after. Therefore, precipitation measurements are temporally offset by 6 hours.

3.3.2 Modeled

Meteorological data from the AROME-Arctic model were to provide a spatially broader view of weather events than can be provided by the point-measurements from the AWS. The AROME-Arctic model is a regional short-range high-resolution forecasting system for the European Arctic with a 2.5 km grid resolution developed by the Norwegian Meteorological Institute (Køltzow et al., 2019; Müller et al., 2017). Forecasted surface variables (e.g., 2 m temperature, 2 m humidity) are interpolated over the grid based on optimal interpolation (Giard & Bazile, 2000). Alexander et al. (2020) validated the forecasted weather with observed weather for the Svalbard airport for the observation periods in 2016 and 2019. The airport observations show good agreement with the closest grid point of the model in the general trends of both air temperature and rainfall. Here we used hourly model data to calculate average daily temperature and net precipitation. Because we present daily average results, it is possible to have liquid rain on a day when the daily average temperature is below zero.

3.4 Satellite data

In addition to point-observations of rain and warm events from the AWSs, and regional model results, we also show remotely sensed rain in synthetic aperture radar (SAR) data following methods from Winsvold et al. (2018). For the study period, Sentinel-1 A radar images (from orbit 37 with a repeat cycle of 12 days) were converted to radiometrically calibrated backscatter images. We applied a backscatter terrain correction using the digital elevation model ASTER 1sec GDEM, and then converted the linear backscatter values to decibels (dB; Figure 3a-e).

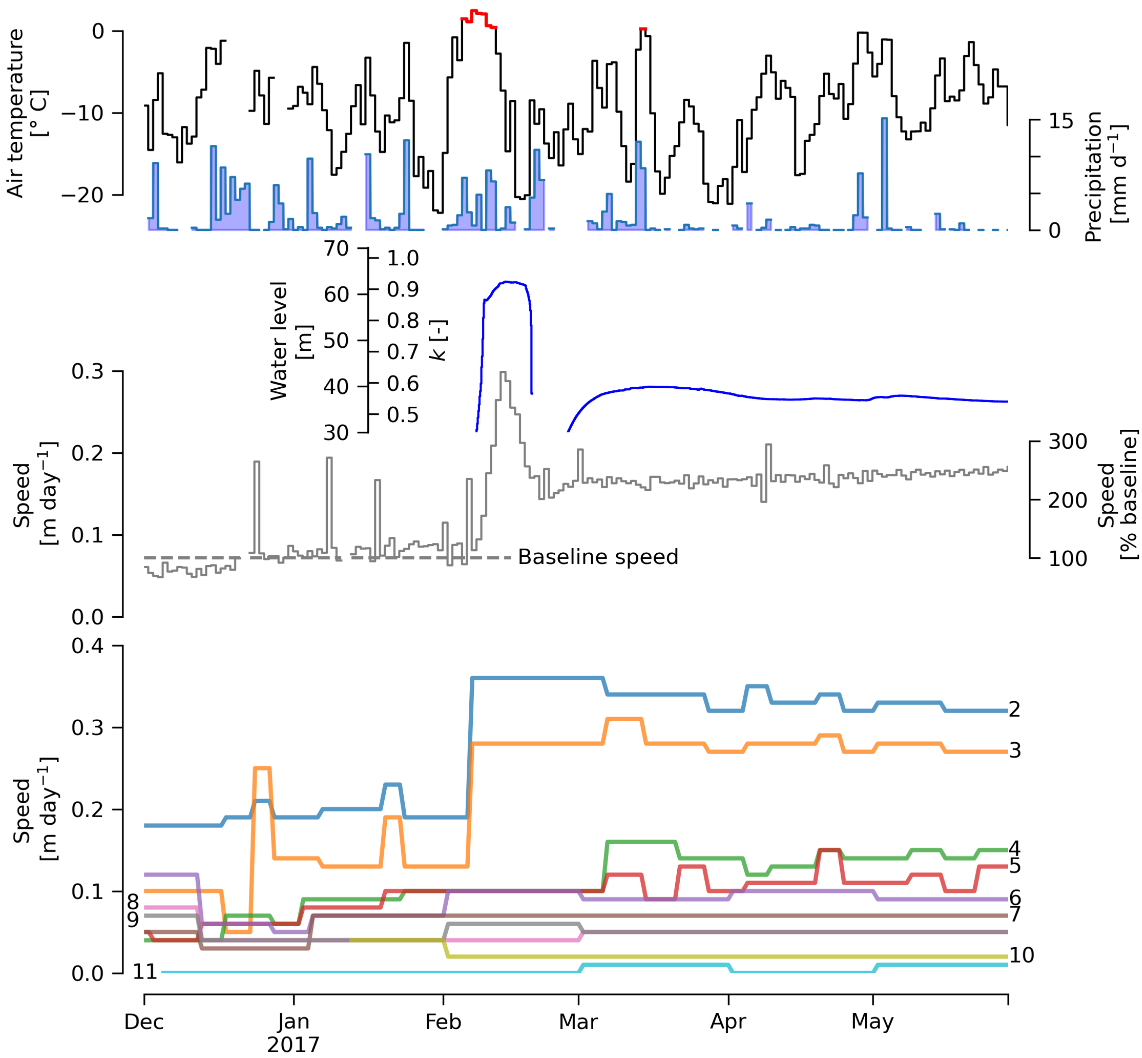

Figure 2. Time series of air temperature at AWS1 (positive red line and negative black line), precipitation (solid, mixed and liquid) at AWS2 (blue area), water level above the bedrock at CC and flotation fraction (k) (blue line) glacier speed at 4MONIT stake (grey line), and glacier speed at all other stakes (bottom panel) during the winter 2016/2017.

4 Results

During our study period, from 2016-12-01 through 2017-05-29, daily average temperatures recorded at AWS1 were below 0° C except for two periods, of which only one was longer than two days. From AWS2 and AROME-Arctic model, both of these warm events included rainfall events (Figures 2 and 3).

4.1 Temperature and hydrology

We highlight the week-long warm period (6 days 20 hours and 30 minutes) with a maximum of 3° C and mean of 1.5° C in early February 2017 (Figure 2). During this period, rain fell over the entire glacier surface (Figure 3). Prior to this warm event, the glacier surface is relatively dry (Figure 3a,b), and water level was below the sensor (less than 28 m above the bed) and therefore not shown in figure 2. On 16 February 2017, five days after the winter melt/rainfall event, the entire glacier surface is wetter (Figure 3c). Beginning 64.5 hours after the first melt day (temperature > 0° C) water rose over 3 days to more than 60 m above the glacier bed, remained there for more than 9 days, then rapidly dropped below the sensor for about 7 days, and returned to a level around 38 m above the bedrock (k around 0.55), and remained there for the duration of the record, until June 2017 (Figure 2). Several weeks after the warm event, the glacier surface is drier (Figure 3d, e).

4.2 Velocity

The velocity record at 4MONIT begins at ca. 0.07 m day^{-1} and climbs slowly to just under 0.1 m day^{-1} from 1 December 2016 through 10 February 2017. Coincident with the water level increase, velocity increased to more than 400 % of the baseline velocity, then dropped to ca. 200 % and then remained near 250 % of the baseline velocity for the duration of the record, until June 2017.

The lower ablation area of the glacier (stakes 2 through 4) reacted similarly to stake 4MONIT (Figure 2). The upper ablation area (stakes 5 through 7) also exhibited an increase in average winter velocity after the warm event. The accumulation area (stakes 8 to 11) did not respond to the event (Figure 2).

5 Discussion

Because of the length of Arctic winter vs. summer the annual velocity is primarily controlled by the winter velocity (Table 1). Therefore, persistent high winter velocities represent a substantial dynamic response and potential significant source of additional sea level rise. The occurrence of winter warm events (Pitcher et al., 2020; Wu, 2017) and winter rain events (Nowak & Hodson, 2013) in the Arctic is increasing (Graham et al., 2017; Łupikasza et al., 2019; Moore, 2016; Peeters et al., 2019; Sobota et al., 2020; Vikhamar-Schuler et al., 2016). Winter warm events may have a larger influence on the annual average velocity of the glacier than a warm event or a rain event in summer - in the case presented here, a brief winter warm event increased glacier velocity more than 200 % over the baseline velocity for several months. Until enough winter water enters the glacier system to cause efficient drainage channels, it is likely that small volumes of winter water, spread over the entire glacier, will act analogous to a "spring event", inducing an increase in ice velocity (Bingham et al., 2006; Kessler & Anderson, 2004; Mair et al., 2003), with no subsequent decrease, as shown here. This persistent doubling velocity from the baseline only occurs in the ablation area (Figure 2), as the IDS does not exist in the accumulation area (Decaux et al., 2019).

The winter warm event described here supplied the entire glacier with a both meltwater and rain (Figure 2 and 3) resulting in wetting of the entire glacier surface (Figure 3c). We are not able to determine using the SAR images if the lowermost part of Hansbreen has been influenced by this event (Figure 3c) due to crevasses causing an increase in backscatter coefficient (Forster et al., 1996). After the warm event and coincident rise in water level (Figure 2), the water briefly drops below the sensor (< 28 m above the bed), then returns to 38 m above the bed, followed by a slight decrease in water level and slight increase in velocity. We hypothesize that the volume of meltwater generated by the warm event was large enough to briefly reopen the IDS. If so, then some water likely evacu-

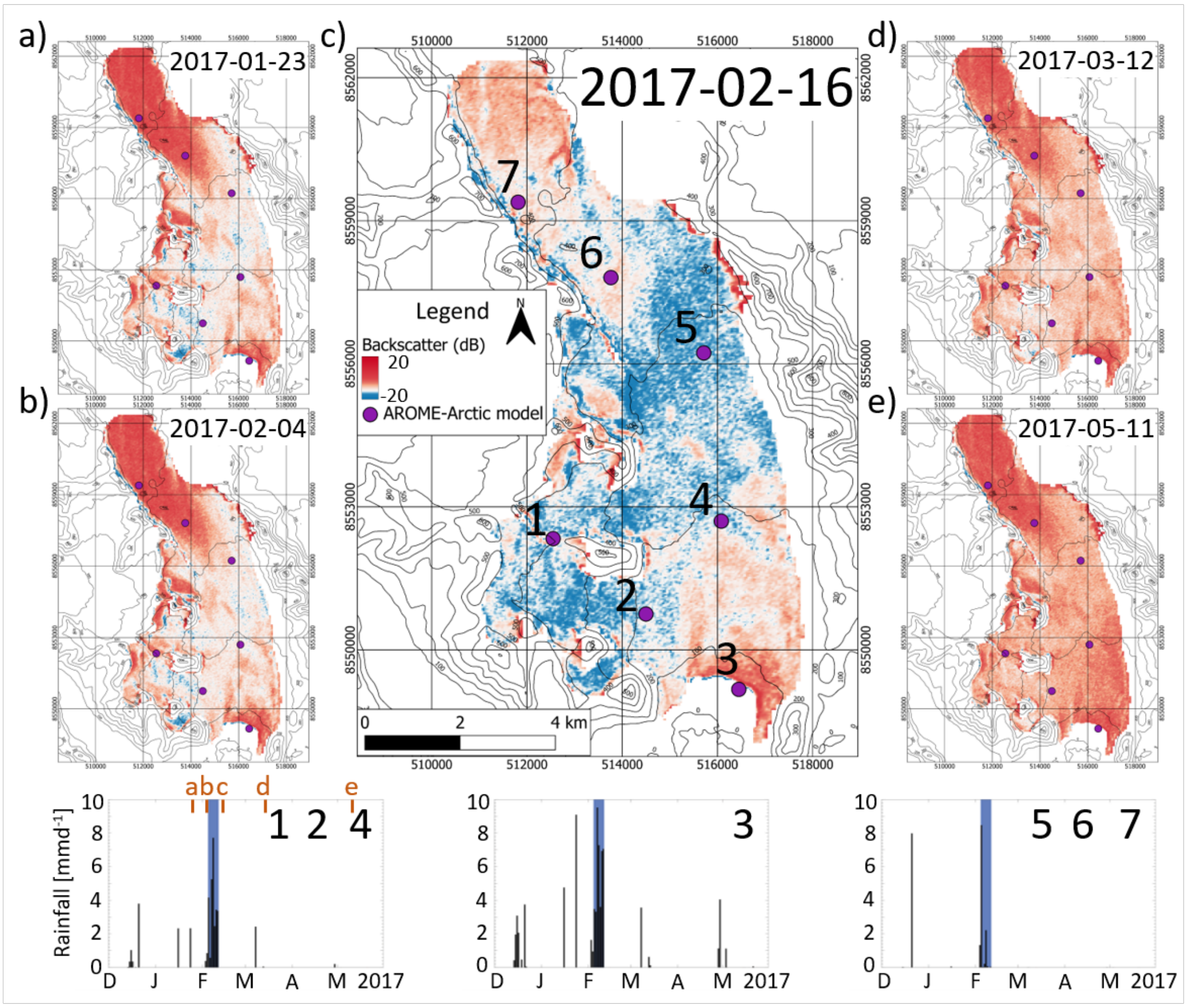

Figure 3. Sentinel-1A backscatter (dB) images from five different days for Hansbreen (a-e). Blue color indicates lower backscatter values showing wetter conditions. The three graphics represent the rainfall modeled by the AROME-Arctic model for seven locations shown on the map (c) by the corresponding numbered purple points for the study period. Winter melt event studied is highlighted in blue on each time series and images (a-e) are placed on the timeline of the first panel.

	Stake 3	Stake 4	Stake 5
Annual (2009-18)	0.37	0.21	0.15
Winter (2009-18)	0.36	0.20	0.15
Summer (2009-18)	0.40	0.22	0.17

Table 1. 10 years average velocity for stakes 3, 4 and 5 in m.d-1. Winter represents the period from October to May and summer the period from June to September.

ated out the glacier front, after which the remaining water was captured within in the IDS due to creep-closure of subglacial channels (Duval, 1977; Duval et al., 1983; Glen, 1955). It is likely creep closure explains the 10 m water level increase (from the sensor at 28 m above the bed to the final ca. 38 m above the bed; Figure 2) observed at the end of February. This upwelling, together with a re-pressurisation of the subglacial system, explains the velocity increases (Davison et al., 2019). After this upwelling ends in early March, the slow decrease in water level is due to water leaving this cave system. It is not likely that water is directly draining out the front of the glacier into the fjord, because a decrease in subglacial water volume would likely cause a decrease in ice velocity, not an increase as shown here. Therefore, the local decrease in water level is likely due to creep closure of the system, pushing water to the surrounding bed, and decreasing the effective pressure (Cowton et al., 2016; I. J. Hewitt, 2011; Werder et al., 2013), after which it may or may not leave the glacier. Water transfer from a channelized system to the surrounding bed increases the water pressure within the distributed system at the base of the glacier, leading to an increase in ice velocity (Cowton et al., 2016; Mair et al., 2002). This warm winter event may have also influenced the velocity of the following 2017 summer, which had an average near-terminus velocity 18 % higher than the last 10 years (0.47 m.d^{-1} compare to 0.40 m d^{-1}) (Table 1).

If we assume stake 2 as representative of the front velocity (Figure 1a), its winter baseline velocity (from 2016-12-01 to 2017-02-01) is ca. 0.19 m day^{-1}. After the warm winter event its average velocity is ca. 0.34 m day^{-1} until the end of the accumulation season (end of May). The velocity increase from this warm event, lasting more than 3 months, is ca. 0.15 m day^{-1}. If the ice front did not move and velocity can be directly related to calving, then 80 % more ice entered the fjord in the 2016/2017 winter than if this 1-week warm event had not occurred, or ca. 20 % (ca. 5 Mt) more ice compared to the annual average. Here the annual increase is only 20 % from the 80 % winter increase, because the anomaly only occurs for 3 winter months.

Data gaps and velocity spikes - We show two gaps in the temperature record (duration of 6 days and 5 days), due to a sensor malfunction, during which precipitation events occur in December 2016 (Figure 2). There is no observed water level fluctuations (water level remained within 28 m of the bed) and no coincident velocity increase. Therefore, we assume that temperatures remain below 0° C. In addition, there are 3 one-day-long velocity increases prior to the February event, with coincident AROME-Arctic model rain events (Figure 3). We assume the cause of these short-term velocity increases is from these rain events. However, they have no lasting impact observed in our data.

Our dataset also highlights winter water storage with implications for observed winter discharge (e.g., Hodge, 1974; Hodgkins, 1997; Hodson et al., 2005; Jansson et al., 2003; Wadham et al., 2000). Our observed water level remains more or less steady at 38 m above the bedrock with k values around 0.55 (Figure 2), providing evidence of multi-month storage of large volumes of water. However, water can move dynamically and discharge to the distributed system, from the channelized one, while appearing more or less steady at the location of the logger, if the subglacial system closes equal to the volume discharged. We note that Pitcher et al. (2020) attribute their winter Greenland glacier discharge to storage of summer runoff, but acknowledge a warm event 10 days prior to their one day observation. Our data suggests that winter warm events may fill the system and could be the cause of winter discharge.

Similarly, Vijay et al. (2019) identified “type-3” glaciers in Greenland which are characterized by winter speedup events associated with subglacial meltwater activity. They assign the meltwater to different sources: basal meltwater, ocean water infiltrating into the subglacial system, and meltwater that did not evacuate through channels during the melt season and was retained in the firn and ice body. We suggest that in addition to these sources, winter warm events of which there are an increasing number in Greenland (Oltmanns et al., 2019), may create “type-3” glaciers.

The observations here are not unique to this glacier or Svalbard. After a warm winter event in Iceland, a Glacsweb wireless probe installed at the Skálafellsjökull glacier bed by Hart et al. (2019) observed a similar water pressure pattern. After an initial water pressure increase attributed to the warm winter event, they recorded a sharp water pressure decline followed by a slow rise on subsequent days until the next melt event (Hart et al., 2019). Other Arctic glaciers may also be susceptible to these events. As the climate warms, precipitation onto the Greenland ice sheet is likely to shift towards a higher fraction of rain in the total precipitation (Bintanja & Andry, 2017; Boisvert et al., 2018; Lenaerts et al., 2020; Screen & Simmonds, 2012). If glacier dynamics models do not take into account the increase in off-season rain shown by regional climate models, then they may not properly model the magnitude of dynamic changes, with related limitations in their ability to properly estimate sea level rise.

6 Conclusions

We show an Arctic glacier, as a result of a single week-long winter warm event, has its average winter velocity in the ablation area more than quadruple (temporarily) and remain at more than double the baseline for the remainder of the winter. The velocity increase appears to be sustained by englacial and subglacial water storage. Within 10 days of the event a nearly steady state is reached, albeit with a small decrease in water level and continued small increase in ice velocity for the remainder of the winter. We attribute this to water transfer out of subglacial conduits to the distributed system at the base of the glacier.

Warm winter events in the Arctic are being reported more often, and predicted to occur more often in a warming climate. We show these warm events can lead to large and sustained increases in ice velocity. Arctic tidewater glaciers are currently the most significant contributor to eustatic sea level rise. Further studies linking the atmosphere, ice velocity, and the winter subglacial hydrologic system are needed to quantify this contribution to sea level rise.

Acknowledgments

Data Availability Statement

All the data are archived at the Polish Polar Data Base: `http://ppdb.us.edu.pl/geonetwork/srv/eng/catalog.search#/home`. Velocity data of 4MONIT stake and of the center line of Hansbreen are respectively available at `http://ppdb.us.edu.pl/geonetwork/srv/eng/catalog.search#/metadata/6e8f320d-4c06-40ce-86cc-f8561d3df4bb` and `http://ppdb.us.edu.pl/geonetwork/srv/eng/catalog.search#/metadata/8c5219c5-2adb-40a5-a9de-eedcf8d0c7da`. Air temperature and precipitation are respectively available at `http://ppdb.us.edu.pl/geonetwork/srv/eng/catalog.search#/metadata/e5e66a63-126d-49e1-bebe-c623becfb5d8` and `http://ppdb.us.edu.pl/geonetwork/srv/eng/catalog.search#/metadata/6603c86f-3194-4fbd-a7e8-5c0bbf430c94`. Water level data of C.C are available at `http://ppdb.us.edu.pl/geonetwork/srv/eng/catalog.search#/metadata/0a4570d3-576b-45e7-947e-737f610d976f`.

This work has been financed by the Centre for Polar Studies, University of Silesia – the Leading National Research Centre (KNOW) in Earth Sciences (2014–2018), No. 03/KNOW2/2014. Glaciological, hydrological and meteorological data were processed by the University of Silesia data repository within project Integrated Arctic Observing System (INTAROS). This project has received funding from the European Union's Horizon 2020 research and innovation programme under grant agreement no. 727890. Instrumentation was funded by the National Geographic Committee for Research and Exploration Grant 9768-15. We wish to thank colleagues from the Polish Polar Station at Hornsund and the Institute of Geophysics Polish Academy of Sciences for hospitality and logistic support during field missions. Access to the meteorological data from the Hornsund station and GNSS data provided by the Institute of Geophysics, Polish Academy of Sciences is kindly acknowledged. The study used equipment and logistical resources belonging to the Polar Laboratory of the University of Silesia in Katowice. Thanks to the VENDYS foundation for its support. Thanks to Barbara Barzycka for providing data on ELA. Léo Decaux acknowledges the field assistance of Anton Sedlák, Kacper Konior, Jakub Medrzycki, Andreas Alexander, Konrad Osienienko, Sabina Kucieba, Kamil Pałkowski, Mateusz Mandat, Mariusz Czarnul, Maciej Błaszkowski, Robert Pogorzelski, Dominika Dabrowska, Grzegorz Piotrowski, Benita Siepierska, Jakub Szewczyk, Bartosz Siek and Łukasz Pawłowski. There are no conflicts of interest.

References

Alexander, A., Obu, J., Schuler, T. V., Kääb, A., & Christiansen, H. H. (2020). Subglacial permafrost dynamics and erosion inside subglacial channels driven by surface events in svalbard. *The Cryosphere*, *14*(11), 4217–4231.

Anderson, Anderson, S. P., MacGregor, K. R., Waddington, E. D., O'Neel, S., Riihimaki, C. A., & Loso, M. G. (2004). Strong feedbacks between hydrology and sliding of a small alpine glacier. *Journal of Geophysical Research: Earth Surface*, *109*(F3).

Anderson, Willis, I., Goodsell, B., Banwell, A., Owens, I., Mackintosh, A., & Lawson, W. (2014). Annual to daily ice velocity and water pressure variations on ka roimata o hine hukatere (franz josef glacier), new zealand. *Arctic, Antarctic, and Alpine Research*, *46*(4), 919–932.

Bartholomaus, T. C., Anderson, R. S., & Anderson, S. P. (2008). Response of glacier basal motion to transient water storage. *Nature Geoscience*, *1*(1), 33–37.

Benn, D., Gulley, J., Luckman, A., Adamek, A., & Glowacki, P. S. (2009). Englacial drainage systems formed by hydrologically driven crevasse propagation. *Journal of Glaciology*, *55*(191), 513–523.

Bingham, R. G., Nienow, P. W., Sharp, M. J., & Copland, L. (2006). Hydrology and dynamics of a polythermal (mostly cold) high arctic glacier. *Earth Surface Processes and Landforms: The Journal of the British Geomorphological Research Group*, *31*(12), 1463–1479.

Bintanja, R., & Andry, O. (2017). Towards a rain-dominated arctic. *Nature Climate Change*, *7*(4), 263–267.

Błaszczyk, M., Jania, J. A., & Hagen, J. O. (2009). Tidewater glaciers of svalbard: Recent changes and estimates of calving fluxes. *Polish Polar Research*, *30*(2), 85–142.

Boisvert, L. N., Webster, M. A., Petty, A. A., Markus, T., Bromwich, D. H., & Cullather, R. I. (2018). Intercomparison of precipitation estimates over the arctic ocean and its peripheral seas from reanalyses. *Journal of Climate*, *31*(20), 8441–8462.

Brinkerhoff, D. J., Meyer, C. R., Bueler, E., Truffer, M., & Bartholomaus, T. C. (2016). Inversion of a glacier hydrology model. *Annals of Glaciology*, *57*(72), 84–95.

Burgess, E. W., Larsen, C. F., & Forster, R. R. (2013). Summer melt regulates winter glacier flow speeds throughout alaska. *Geophysical Research Letters*, *40*(23), 6160–6164.

Chen, Y., Liu, X., Gulley, J. D., & Mankoff, K. D. (2018, 10). Subglacial conduit roughness: Insights from computational fluid dynamics models. *Geophysical Research Letters*, *45*(20), 11,206–11,218. doi: 10.1029/2018gl079590

Cowton, T., Nienow, P., Sole, A., Bartholomew, I., & Mair, D. (2016). Variability in ice motion at a land-terminating greenlandic outlet glacier: the role of channelized and distributed drainage systems. *Journal of Glaciology*, *62*(233), 451–466.

Davison, B. J., Sole, A. J., Livingstone, S. J., Cowton, T. R., & Nienow, P. W. (2019). The influence of hydrology on the dynamics of land-terminating sectors of the greenland ice sheet. *Frontiers in Earth Science*, *7*, 10.

Decaux, L., Grabiec, M., Ignatiuk, D., & Jania, J. (2019). Role of discrete water recharge from supraglacial drainage systems in modeling patterns of subglacial conduits in svalbard glaciers. *The Cryosphere*, *13*(3), 735–752.

Doyle, S. H., Hubbard, A., Van De Wal, R. S., Box, J. E., Van As, D., Scharrer, K., ... Hubbard, B. (2015). Amplified melt and flow of the greenland ice sheet driven by late-summer cyclonic rainfall. *Nature Geoscience*, *8*(8), 647–653.

Duval, P. (1977). The role of the water content on the creep rate of polycrystalline ice. *IAHS Publ*, *118*, 29–33.

Duval, P., Ashby, M., & Anderman, I. (1983). Rate-controlling processes in the creep of polycrystalline ice. *The Journal of Physical Chemistry*, *87*(21), 4066–4074.

Flowers, G. E., & Clarke, G. K. (1999). Surface and bed topography of trapridge glacier, yukon territory, canada: digital elevation models and derived hydraulic geometry. *Journal of Glaciology*, *45*(149), 165–174.

Forster, R. R., Isacks, B. L., & Das, S. B. (1996). Shuttle imaging radar (sir-c/x-sar) reveals near-surface properties of the south patagonian icefield. *Journal of Geophysical Research: Planets*, *101*(E10), 23169–23180.

Giard, D., & Bazile, E. (2000). Implementation of a new assimilation scheme for soil and surface variables in a global nwp model. *Monthly weather review*, *128*(4), 997–1015.

Glen, J. W. (1955). The creep of polycrystalline ice. *Proceedings of the Royal Society of London. Series A. Mathematical and Physical Sciences*, *228*(1175), 519–538.

Grabiec, M., Jania, J., Puczko, D., Kolondra, L., & Budzik, T. (2012). Surface and bed morphology of hansbreen, a tidewater glacier in spitsbergen. *Polish Polar Research*, *33*(2), 111–138.

Graham, R. M., Cohen, L., Petty, A. A., Boisvert, L. N., Rinke, A., Hudson, S. R., ... Granskog, M. A. (2017). Increasing frequency and duration of arctic winter warming events. *Geophysical Research Letters*, *44*(13), 6974–6983.

Gulley, J. D., Grabiec, M., Martin, J. B., Jania, J., Catania, G. A., & Głowacki, P. (2012). The effect of discrete recharge by moulins and heterogeneity in flow-path efficiency at glacier beds on subglacial hydrology. *Journal of Glaciology*, *58*(211), 926 – 940. doi: 10.3189/2012JoG11J189

Gulley, J. D., Spellman, P. D., Covington, M. D., Martin, J. B., Benn, D. I., & Catania, G. A. (2014). Large values of hydraulic roughness in subglacial conduits during conduit enlargement: Implications for modeling conduit evolution. *Earth Surface Processes and Landforms*, *39*(3), 296–310. doi: 10.1002/esp.3447

Hagen, J. O., Kohler, J., Melvold, K., & Winther, J.-G. (2003). Glaciers in svalbard: mass balance, runoff and freshwater flux. *Polar Research*, *22*(2), 145–159.

Hagen, J. O., Liestøl, O., Roland, E., & Jørgensen, T. (1993). *Glacier atlas of svalbard and jan mayen.* Norsk Polarinstitutt Oslo.

Harrison, W. D., & Post, A. S. (2003). How much do we really know about glacier surging? *Annals of glaciology*, *36*, 1–6.

Hart, J. K., Martinez, K., Basford, P. J., Clayton, A. I., Robson, B. A., & Young, D. S. (2019). Surface melt driven summer diurnal and winter multi-day stick-slip motion and till sedimentology. *Nature communications*, *10*(1), 1–11.

Hewitt, I. (2013). Seasonal changes in ice sheet motion due to melt water lubrication. *Earth and Planetary Science Letters*, *371*, 16–25.

Hewitt, I. J. (2011). Modelling distributed and channelized subglacial drainage: the spacing of channels. *Journal of Glaciology*, *57*(202), 302–314.

Hodge, S. M. (1974). Variations in the sliding of a temperate glacier. *Journal of Glaciology*, *13*(69), 349–369.
Hodgkins, R. (1997). Glacier hydrology in svalbard, norwegian high arctic. *Quaternary Science Reviews*, *16*(9), 957–973.
Hodson, A., Kohler, J., Brinkhaus, M., & Wynn, P. (2005). Multi-year water and surface energy budget of a high-latitude polythermal glacier: evidence for overwinter water storage in a dynamic subglacial reservoir. *Annals of Glaciology*, *42*, 42–46.
Hooke, R. L., Hanson, B., Iverson, N. R., Jansson, P., & Fischer, U. H. (1997). Rheology of till beneath storglaciären, sweden. *Journal of Glaciology*, *43*(143), 172–179.
Iken, A., & Bindschadler, R. A. (1986). Combined measurements of subglacial water pressure and surface velocity of findelengletscher, switzerland: conclusions about drainage system and sliding mechanism. *Journal of Glaciology*, *32*(110), 101–119.
Jania, J., Macheret, Y. Y., Navarro, F., Glazovsky, A., Vasilenko, E., Lapazaran, J., ... Piwowar, B. (2005). Temporal changes in the radiophysical properties of a polythermal glacier in spitsbergen. *Annals of Glaciology*, *42*, 125–134.
Jansson, P. (1995). Water pressure and basal sliding on storglaciären, northern sweden. *Journal of Glaciology*, *41*(138), 232–240.
Jansson, P., Hock, R., & Schneider, T. (2003). The concept of glacier storage: a review. *Journal of Hydrology*, *282*(1-4), 116–129.
Joughin, I., Das, S. B., King, M. A., Smith, B. E., Howat, I. M., & Moon, T. (2008). Seasonal speedup along the western flank of the greenland ice sheet. *Science*, *320*(5877), 781–783.
Kamb, B., Raymond, C., Harrison, W., Engelhardt, H., Echelmeyer, K., Humphrey, N., ... Pfeffer, T. (1985). Glacier surge mechanism: 1982-1983 surge of variegated glacier, alaska. *Science*, *227*(4686), 469–479.
Kessler, M. A., & Anderson, R. S. (2004). Testing a numerical glacial hydrological model using spring speed-up events and outburst floods. *Geophysical Research Letters*, *31*(18).
Køltzow, M., Casati, B., Bazile, E., Haiden, T., & Valkonen, T. (2019). An nwp model intercomparison of surface weather parameters in the european arctic during the year of polar prediction special observing period northern hemisphere 1. *Weather and Forecasting*, *34*(4), 959–983.
Lenaerts, J., Camron, M. D., Wyburn-Powell, C. R., & Kay, J. E. (2020). Present-day and future greenland ice sheet precipitation frequency from cloudsat observations and the community earth system model. *The Cryosphere*, *14*(7), 2253–2265.
Lingle, C. S., & Fatland, D. R. (2003). Does englacial water storage drive temperate glacier surges? *Annals of Glaciology*, *36*, 14–20.
Łupikasza, E. B., Ignatiuk, D., Grabiec, M., Cielecka-Nowak, K., Laska, M., Jania, J., ... Budzik, T. (2019). The role of winter rain in the glacial system on svalbard. *Water*, *11*(2), 334.
Mair, D., Nienow, P., Sharp, M., Wohlleben, T., & Willis, I. (2002). Influence of subglacial drainage system evolution on glacier surface motion: Haut glacier d'arolla, switzerland. *Journal of Geophysical Research: Solid Earth*, *107*(B8), EPM–8.
Mair, D., Willis, I., Fischer, U. H., Hubbard, B., Nienow, P., & Hubbard, A. (2003). Hydrological controls on patterns of surface, internal and basal motion during three "spring events": Haut glacier d'arolla, switzerland. *Journal of Glaciology*, *49*(167), 555–567.
Mankoff, K. D., Gulley, J. D., Tulaczyk, S. M., Covington, M. D., Liu, X., Chen, Y., ... Głowacki, P. S. (2017). Roughness of a subglacial conduit under Hansbreen, Svalbard. *Journal of Glaciology*, *63*(239), 423–435. doi:

10.1017/jog.2016.134
Moore, G. (2016). The december 2015 north pole warming event and the increasing occurrence of such events. *Scientific Reports*, *6*(1), 1–11.
Müller, M., Homleid, M., Ivarsson, K.-I., Køltzow, M. A., Lindskog, M., Midtbø, K. H., ... others (2017). Arome-metcoop: A nordic convective-scale operational weather prediction model. *Weather and Forecasting*, *32*(2), 609–627.
Nowak, A., & Hodson, A. (2013). Hydrological response of a high-arctic catchment to changing climate over the past 35 years: a case study of bayelva watershed, svalbard. *Polar Research*, *32*(1), 19691.
Oltmanns, M., Straneo, F., & Tedesco, M. (2019). Increased greenland melt triggered by large-scale, year-round cyclonic moisture intrusions. *The Cryosphere*, *13*(3), 815–825.
Pälli, A., Moore, J. C., Jania, J., Kolondra, L., & Glowacki, P. (2003). The drainage pattern of hansbreen and werenskioldbreen, two polythermal glaciers in svalbard. *Polar Research*, *22*(2), 355–371.
Peeters, B., Pedersen, Å. Ø., Loe, L. E., Isaksen, K., Veiberg, V., Stien, A., ... Hansen, B. B. (2019). Spatiotemporal patterns of rain-on-snow and basal ice in high arctic svalbard: detection of a climate-cryosphere regime shift. *Environmental Research Letters*, *14*(1), 015002.
Pitcher, L. H., Smith, L. C., Gleason, C. J., Miège, C., Ryan, J. C., Hagedorn, B., ... Forster, R. R. (2020). Direct observation of winter meltwater drainage from the greenland ice sheet. *Geophysical Research Letters*, *47*(9), e2019GL086521.
Schoof, C. (2010). Ice-sheet acceleration driven by melt supply variability. *Nature*, *468*(7325), 803–806.
Schoof, C., Rada, C., Wilson, N., Flowers, G., & Haseloff, M. (2014). Oscillatory subglacial drainage in the absence of surface melt. *The Cryosphere*, *8*(3), 959–976.
Schroeder, J. (1998a). Hans glacier moulins observed from 1988 to 1992, svalbard. *Norwegian Journal of Geography*, *52*(2), 78–88.
Schroeder, J. (1998b). Indications of climate change from moulin evolution. *Salzburger Geographische Materialien*, *28*, 27–33.
Schroeder, J. (2007). Moulins of a subpolar glacier seen as a thermal anomaly. In *Karst and cryokarst: Joint proceedings of the 25th speleological school and 8th international glackipr symposium* (pp. 65–74).
Screen, J. A., & Simmonds, I. (2012). Declining summer snowfall in the arctic: Causes, impacts and feedbacks. *Climate dynamics*, *38*(11-12), 2243–2256.
Sobota, I., Weckwerth, P., & Grajewski, T. (2020). Rain-on-snow (ros) events and their relations to snowpack and ice layer changes on small glaciers in svalbard, the high arctic. *Journal of Hydrology*, *590*, 125279.
Sole, A., Nienow, P., Bartholomew, I., Mair, D., Cowton, T., Tedstone, A., & King, M. A. (2013). Winter motion mediates dynamic response of the greenland ice sheet to warmer summers. *Geophysical Research Letters*, *40*(15), 3940–3944.
Stevens, L. A., Behn, M. D., Das, S. B., Joughin, I., Noël, B. P., van den Broeke, M. R., & Herring, T. (2016). Greenland ice sheet flow response to runoff variability. *Geophysical Research Letters*, *43*(21), 11–295.
Sund, M., Lauknes, T. R., & Eiken, T. (2014). Surge dynamics in the nathorstbreen glacier system, svalbard. *The Cryosphere*, *8*(2), 623–638.
Turu, V. (2012). Surface nmr survey on hansbreen glacier, hornsund, sw spitsbergen (norway). *Landform Analysis*, *21*, 57–74.
Vieli, A., Jania, J., Blatter, H., & Funk, M. (2004). Short-term velocity variations on hansbreen, a tidewater glacier in spitsbergen. *Journal of Glaciology*, *50*(170), 389–398.
Vijay, S., Khan, S. A., Kusk, A., Solgaard, A. M., Moon, T., & Bjørk, A. A. (2019). Resolving seasonal ice velocity of 45 greenlandic glaciers with very high tempo-

ral details. *Geophysical Research Letters*, *46*(3), 1485–1495.
Vikhamar-Schuler, D., Isaksen, K., Haugen, J. E., Tømmervik, H., Luks, B., Schuler, T. V., & Bjerke, J. W. (2016). Changes in winter warming events in the nordic arctic region. *Journal of climate*, *29*(17), 6223–6244.
Wadham, J., Tranter, M., & Dowdeswell, J. (2000). Hydrochemistry of meltwaters draining a polythermal-based, high-arctic glacier, south svalbard: Ii. winter and early spring. *Hydrological Processes*, *14*(10), 1767–1786.
Werder, M. A., Hewitt, I. J., Schoof, C. G., & Flowers, G. E. (2013). Modeling channelized and distributed subglacial drainage in two dimensions. *Journal of Geophysical Research: Earth Surface*, *118*(4), 2140–2158.
Willis, I. C. (1995). Intra-annual variations in glacier motion: a review. *Progress in Physical Geography*, *19*(1), 61–106.
Winsvold, S. H., Kääb, A., Nuth, C., Andreassen, L. M., Van Pelt, W. J., & Schellenberger, T. (2018). Using sar satellite data time series for regional glacier mapping. *The Cryosphere*, *12*(3), 867–890.
Wu, B. (2017). Winter atmospheric circulation anomaly associated with recent arctic winter warm anomalies. *Journal of Climate*, *30*(21), 8469–8479.